

Occupational exposure to graphene and silica nanoparticles. Part I: workplace measurements and samplings

Fabio Boccuni, Riccardo Ferrante, Francesca Tombolini, Claudio Natale, Andrea Gordiani, Stefania Sabella, and Sergio Iavicoli

QUERY SHEET

This page lists questions we have about your paper. The numbers displayed at left are hyperlinked to the location of the query in your paper.

The title and author names are listed on this sheet as they will be published, both on your paper and on the Table of Contents. Please review and ensure the information is correct and advise us if any changes need to be made. In addition, please review your paper as a whole for typographical and essential corrections.

Your PDF proof has been enabled so that you can comment on the proof directly using Adobe Acrobat. For further information on marking corrections using Acrobat, please visit <http://journalauthors.tandf.co.uk/production/acrobat.asp>; <https://authorservices.taylorandfrancis.com/how-to-correct-proofs-with-adobe/>

The CrossRef database (www.crossref.org/) has been used to validate the references.

AUTHOR QUERIES

- Q1** The year for ‘Schinwald et al. 2013’ has been changed to ‘2012’ to match the entry in the references list. Please provide revisions if this is incorrect.
- Q2** Please check whether the edits made to the sentence “As reference instrument, the DM ...” convey the intended meaning, and revise if incorrect.
- Q3** Table 5 is cited in the text but it is not provided in the manuscript. Please check and provide revisions.
- Q4** The year of publication has been updated for the reference ‘Bukowiecki et al. 2002’. Please check.
- Q5** Please provide the publisher location for the reference ‘Ferrante et al. 2019’.
- Q6** The reference ‘Hubbs et al. 2013’ has been updated. Please revise if it is inaccurate.
- Q7** The year of publication has been updated for the reference ‘Jeelani et al. 2020’. Please check.
- Q8** Please note that Figure 2 will be set in black and white in print. Please rephrase the legend so that there is no reference to any colours.
- Q9** Please note that Figure 6 will be set in black and white in print. Please rephrase the legend so that there is no reference to any colours.
- Q10** The funding information provided has been checked against the Open Funder Registry and we failed to find a match. Please check and resupply the funding details if necessary.

ARTICLE



Occupational exposure to graphene and silica nanoparticles. Part I: workplace measurements and samplings

Fabio Bocconi^a, Riccardo Ferrante^a, Francesca Tombolini^a, Claudio Natale^a, Andrea Gordiani^a,
Stefania Sabella^b and Sergio Iavicoli^a

^aDepartment of Occupational and Environmental Medicine, Epidemiology and Hygiene, Italian Workers' Compensation Authority (INAIL), Monte Porzio Catone, Rome, Italy; ^bDepartment of Drug Discovery and Development, Italian Institute of Technology (IIT), Genova, Italy

ABSTRACT

Few-Layers Graphene (FLG) are able to improve the performance of materials, due to their chemical-physical properties. Engineered amorphous silica nanoparticles (SiO₂NPs) are among the most widespread nanomaterials (NMs) in the world. Such nanomaterials are two case studies of the research project 'NanoKey' that integrated the exposure assessment through personal measurements and sampling in the workplace, as described in the present work (part I), with the biomonitoring of exposed workers (reported in part II). Measurement campaigns were conducted according to OECD and WHO harmonized approach in two production sites. The set of instruments included real-time devices for high-resolution measurements at the nanoscale and time-integrated samplers for the off-line gravimetric analysis and chemical and morphological (SEM-EDS) characterization of exposure in order to identify the contribution of production compared to the background. Values of particle number concentration (PNC) and lung deposited surface area (LDSA) within the FLG production resulted higher than the background far field (FF), even if they are always similar to the near field (NF) ones: the average diameter (D_{avg}) during the production was higher than the NF background but always lower than the FF values. SEM-EDS analysis highlighted the presence of structures comparable to those produced. During the SiO₂NPs production, the PBZ values showed PNC and LDSA levels higher than the background, with a decrease in the D_{avg} probably due to NPs emission. SEM-EDS confirms the presence of rare silica nanoparticles. Since the exposure to airborne NMs cannot be excluded in both production sites, a prevention-through-design approach to mitigate the potential risk for workers has been recommended.

ARTICLE HISTORY

Received 18 June 2020
Revised 6 October 2020
Accepted 6 October 2020

KEYWORDS

Nanotechnology; nanomaterials; workers; risk assessment; prevention-through-design



Introduction


In recent years nanotechnology showed a rapid development in a wide range of sectors, thanks to the new properties that hallowed multidisciplinary relevance to the materials at the nanoscale. Innovative chemical and physical properties of nanomaterials (NMs), such as graphene (Novoselov et al. 2004), are useful to improve the performance of pristine materials in which they are added (Li et al. 2019). Amorphous silica nanoparticles (SiO₂ NPs) are widespread used in different sectors, from medicine and pharmaceuticals (Jeelani et al. 2020) to the construction industry (Pacheco-Torgal et al. 2019).

In parallel with the production and use of different NMs, researchers focused their interest in the

potential impact for workers involved in industrial and small-scale research and development (R&D) processes. Several scientific studies highlighted that NMs can be more hazardous than the same materials in the bulk form (Oberdorster, Oberdorster, and Oberdorster 2005) also due to the large effective surface area per mass unit (Hubbs et al. 2013).

Scientific studies regarding in vitro and in vivo toxicity assessment of carbon-based NMs, such as Single or Multi Walled Carbon Nanotubes, demonstrate that they cause germ cell mutagenicity, specific organ toxicity, eye damage and carcinogenicity after repeated exposure (Shvedova et al. 2016). At present, many R&D facilities started the production of graphene, few-layers graphene (FLG), graphene

CONTACT Fabio Bocconi  f.bocconi@inail.it  Department of Occupational and Environmental Medicine, Epidemiology and Hygiene, Via Fontana Candida 1, 00078 Monte Porzio Catone, Rome, Italy

 Supplemental data for this article can be accessed [here](#).

© 2020 Informa UK Limited, trading as Taylor & Francis Group

oxide, reduced graphene oxide and graphene nanoplatelets (Fadeel et al. 2018). The nanoscale size and the 2-D dimensionality, represent key parameters for risk analysis of exposure to such graphene-based NMs (Schinwald et al. 2012).

Q1 Toxicological effects are also associated to SiO₂ NPs exposure in the workplace: such nanoscale materials generally exhibit acute toxic effects in vitro and in vivo. The data on chronic effects of exposure are rather conflicting with the acute effects and are still not enough to draw firm conclusions. Moreover, effects on human health remain unclear due to the lack of realistic exposure and epidemiological data (Murugadoss et al. 2017). A recent review on epidemiological findings on workers exposed to synthetic SiO₂ NPs, concluded that the mechanisms of toxicity are the generation of reactive oxygen species and oxidative injury, confirmed also by animal models; pathological alterations occurred in workers exposed not wearing personal protective equipment (Schulte et al. 2019).

As long as specific occupational exposure limits (OELs) for NMs will be not applicable in workplaces, the World Health Organization (WHO 2017) proposed to follow a stepwise approach for measurement of exposure by inhalation: first, an assessment of the potential for exposure; second, conducting a basic exposure assessment and third, conducting a comprehensive exposure assessment according to the guidelines proposed by the Organization for Economic Cooperation and Development (OECD 2015, 2017).

Although the emission potential parameters alone do not predict the worker exposure potential (Bergamaschi et al. 2015), the integration of exposure measurements and sampling with the bio-monitoring of involved workers may represent an added value for a comprehensive occupational exposure characterization (Schulte et al. 2018).

In this framework a research project has been developed by the Italian Workers' Compensation Authority (INAIL) with the aim to assess the occupational exposure to different types of NMs, integrating personal and workplace measurements/sampling and biomonitoring of exposed workers. The present study (part I) is focused on the results of the measurements and sampling of airborne FLG and SiO₂ NPs produced in two different facilities in order to characterize the workers' exposure by

inhalation. In the Part II (Ursini et al. 2020) the results of biomonitoring of workers involved in both production processes will be reported.

Materials and methods

Nanomaterials and production processes

The case studies have been identified in two production laboratories of NMs with different properties and dimensionalities:

- 2-D FLG powders are produced in the Facility A, according to the patented protocol of exfoliation of layered materials by Wet-Jet Milling techniques developed by Del Rio Castillo et al. (2016). The final products are in the form of flakes with crystalline nature and lateral dimensions of 100–1000 nm, which can be further functionalized with nitrogen or oxygen atoms.
- 0-D SiO₂ NPs are produced in the Facility B, by synthesis in liquid phase and following washing and drying processes to obtain powders in three different average sizes (25, 50 and 100 nm) and two surface charges (positive and negative) (Malvindi et al. 2012, 2014). During the process monitored in the extensive campaign SiO₂ NPs of average 50 nm size were produced.

Standard process phases of both case studies are summarized in the Table 1; detailed information on materials have been collected by an information data sheet already developed in a previous study (Boccuni et al. 2018), filled in by the manufacturing laboratory for each case study and reported in Supplementary Table S1.

Measurement and sampling approach

The exposure by inhalation has been assessed through measurements and samplings according to the harmonized tiered approach defined by OECD (2015) and recommended by WHO (2017). For both case studies information about processes, operating procedures, workplaces and safety equipment have been reported in Supplementary Table S1.

Preliminary measurements and sampling have been realized during specific walkthrough sessions organized in both facilities in which materials were produced. Laboratory simulations using trial

Table 1. Case studies processes and phases description.

FLG process phases (state of NMs)	Description
A.1. Wet Jet Mill (liquid)	The mixture of graphite layered crystals dispersed in N-methyl-2-pyrrolidone (NMP) is subsequently passed through the 300, 200, 150 and 100 micron nozzle to product 10 L of graphene-based ink at a concentration of 10 g/L. Time averaged duration 8 h.
A.2. Rotovapor (liquid)	Evaporation of graphene-based ink dispersed in NMP (8 L per cycle). Washing with Acetone or Propan-2-ol and re-dispersion in Dimethyl Sulfoxide (DMSO) to obtain the ink at 30 g/L concentration in DMSO. Time averaged duration 8 hours.
A.3. Freeze Drying (powder)	The graphene-based ink in DMSO is firstly frozen and then dried (vacuum sealed) to obtain, at the best, 100 g of graphene-based powder per cycle. Time averaged duration 50 h.
A.4. Storage and Cleaning (powder)	At the end of the phase A.3 the freeze dryers are opened and the Petri dishes (freeze dryer containers) are put under the recirculation hood for the storage. Workers handle about 90 g of FLG during in this step. Time averaged duration 3 hours. During the defrosting process, the freeze dryers are washed with Propan-2-ol or Acetone up to a maximum of 1 L per each freeze dryer. Time averaged duration 15 min. During the phase the air-conditioning system inside the laboratory is turned off, leaving on the local extraction hoods.
SiO ₂ NPs process phases	
B.1. Synthesis (liquid)	10 ml of reagents and solvents in solution are mixed in a stirrer. Time averaged duration 24 h.
B.2. Washing (liquid)	The solution is washed in a spin-drier using ethanol (10 mL) and water. Time averaged duration 1 h.
B.3. Drying (powder)	In this phase the concentration of NPs in water solution is measured and then the materials are converted in powder form inside a dryer. At the end the dryer is open in order to extract the products. During the activities the equipment are cleaned using compressed air. Time averaged duration 24 h.
B.4. Weighting, dilution and storage (powder)	Weighting of powders, using a laboratory scale, and storage. Workers handle about 20 mg of SiO ₂ NPs during in this step. If requested the NPs are also diluted in water solution and stored in this form. Time averaged duration 1 h 30 min.

samples of final materials allowed us to check the sampling strategies and the instruments' responses.

An extensive campaign has been conducted for each case study to monitor all production phases and background levels.

Two approaches for background characterization were used in our study:

- Far-Field (FF) background: measured in the same facility in a location where no NMs are produced, far from the workstations and not influenced by the process. FF background was collected simultaneously with the measurements conducted during the production inside the laboratories.
- Near-Field (NF) approach: background is measured before the production started, inside each laboratory within a range of 1.5 m from the workstations.

Furthermore we measured the worker's personal exposure in the personal breathing zone (PBZ), i.e. within a 0.3 m radius of worker's nose and mouth, before (PBZ background) and during the activities. In the same way, we measured the workplace exposure in the NF location, representing the position of another worker not directly involved in the process phase.

Particle number concentration (PNC) significant values have been calculated based on OECD (2015)

methodology as the average background plus three times the related standard deviation. They represent the values beyond which NMs emission by production may be supposed (Brouwer et al. 2016).

The set of instruments involved in both extensive sampling campaigns was composed by:

- Condensation Particle Counter (CPC mod. 3007, TSI Inc., Shoreview, MN, USA) to measure in real-time the PNC (part/cm³) from 10 to 1,000 nm, with 1 s time resolution (1 Hz) and accuracy $\pm 20\%$ (total flow 0.7 L/min; detection limits 1 to 100,000 part/cm³).
- DiSCmini (DM mod. TESTO SE & Co. KGaA, Germany), handheld instrument for the measurement of personal PNC in the range 10–700 nm, average diameter (D_{avg}) of diffusion charging and Lung Deposited Surface Area (LDSA) in the range 10–300 nm, based on the model published by the International Commission on Radiological Protection (ICRP 1994), with a lower 1 s time resolution. Three different DMs have been used for parallel measurements.
- Fast Mobility Particle Sizer (FMPS mod. 3091, TSI Inc., Shoreview, MN, USA) to measure real-time particle size distribution (PSD, dN/dlogDp) and simultaneously measure total PNC (part/cm³), in the size interval 5.6–560 nm, with 1 s time resolution.

- Nanoparticle Surface Area Monitor (NSAM mod. 3550, TSI Inc., Shoreview, MN, USA) to measure the running average LDSA ($\mu\text{m}^2/\text{cm}^3$) of particles from 10 nm to 1,000 nm, with 1 s time resolution, corresponding to the alveolar pulmonary fraction, based on the ICRP (1994) model.
- Electrical Low Pressure Impactor (ELPI+ mod. Dekati Ltd, Finland) to measure real-time total PNC and PSD in the size range 6–10,000 nm (1 Hz sampling rate) and to collect on plates size classified particles for off-line analysis. Sampling supports are in aluminum (Al) with 25 mm size.
- Photoelectric Aerosol Sensor (PAS2000, EcoChem Analytics, League City, TX USA) to measure polycyclic aromatic hydrocarbons (PAHs) surface-adsorbed on carbon aerosol with aerodynamic diameter from 10 nm to 1,500 nm, with a response time of 10 s in the measuring interval 3–1,000 ng/m^3 .
- Personal samplers (mod. Sioutas, SKC Inc., Eighty Four, PA, USA) equipped with a pump (9 L/min flow) to collect particles from 250 nm to 2500 nm (in five stages: > 2500 (to 10,000), 1,000–2,500, 500–1,000, 250–500 and <250 nm). Sioutas are equipped with Al filters (25 mm) on four stages and polytetrafluoroethylene (PTFE) filters (37 mm) on the backup stage (<250 nm). Four different Sioutas devices have been involved for parallel sampling, two collecting materials for morphological analysis and two for gravimetric analysis.

Off-line analysis of sampled materials has been conducted for a comprehensive characterization of the exposure scenarios:

- Gravimetric analysis has been performed by weighting filters sampled by Sioutas before the sampling and after (average on three weighting operations) by an analytic scale (mod. xs105, resolution = 0.01 μg): mass differences represented to the total airborne particle matter, in the instrumental size ranges.
- Morphological and elemental analyses have been performed on materials collected by Sioutas and ELPI+ to find the presence of the produced NMs in the workplace air and their shapes in the samples, using a High-Resolution Field Emission Scanning Electron Microscope

(HR-SEM) Ultra Plus (ZEISS) equipped with an Energy Dispersive X-ray Spectroscopy (EDS, Oxford Instruments INCA).

- Chemical analysis on cartridge for collection of volatile organic compounds (VOCs) and airborne solvents has been performed in the FLG case, through Gas-Chromatography Mass Spectrometer (GC-MS mod. Agilent Technologies 5975 C-inert MSD).
- VOCs cartridge mod. Anasorb CSC (SKC Inc., 863 Valley View Road, Eighty Four PA 15330 USA) sorbent tube, coconut charcoal, 6 x 70 mm size, 2 sections, 50/100 mg sorbent, 20/40 mesh, with GS ends and FFW separators, fits Type A tube cover, pk/5.

Detailed information about the whole set of instruments used in this study are also reported elsewhere (Ferrante et al. 2019).

Data processing and statistical analysis included real-time values of PNC (both personal and workplace) comparison with significant values in order to identify the process phases with potential emission. PBZ measurements of PNC, D_{avg} and LDSA are compared to the simultaneous NF and FF values with the aim to highlight workers' personal exposure.

PSD (dN/dlogDp) of airborne nanoscale materials has been measured in the background and during the production. Measured values were normalized with respect to the total concentration obtained in the whole sampling period to identify the specific contribution (%) of each size. PSD values obtained from FMPS and ELPI+ have been used also to calculate D_{avg} corresponding value according to Equation (1):

$$D_{\text{avg}}(t) = \frac{\sum_i N_i * d_i}{\sum_i N_i} \quad (1)$$

where N_i is the PNC related to the i^{th} diameter d_i , with i ranging from 5.6 to 560 nm (into the 32 different channels of FMPS) or from 6 to 10,000 nm (into the 14 different channels of ELPI+) (Ramachandran & Cooper 2011).

In the SiO_2 NPs case the PSD obtained from ELPI+ has been used to calculate corresponding LDSA values according to Kuuluvainen et al. (2016), who observed a linear correlation between LDSA measured by NSAM and a function of the ELPI total

current. In the present study such correlation has been calculated in the workplace conditions, obtaining a calibration factor of $40 \mu\text{m}^2/\text{cm}^3\text{pA}$ ($R^2 = 0.97$).

PAHs concentration was monitored by PAS2000 in order to identify environmental pollutants in the workplace air. In addition in the FLG case, PAHs signal may be useful for the identification of elemental carbon (Bukowiecki et al. 2002) during the carbon-based materials production, as already described by Evans et al. (2010).

VOCs samplings were conducted according to the procedures for measurements of chemical agents in the workplace established by the European standard EN 482:2012 (CEN 2012).

Measurement campaigns setting up

FLG production process is developed in a laboratory of area about 43.5 m^2 (Length = 7.5 m Width = 5.8 m and Height = 3.2 m) located at the first underground floor in the Facility A (Figure 1(a)), equipped with mechanical ventilation (6 air change per hour) for air conditioning and a dedicated system including local extraction hoods connected to the aspiration line of exhaust fumes. Personal protective

equipment (PPE) include suits, coats, nitrile gloves, cold resistant gloves, arm sleeves, glasses, masks and ear protection headphones (Supplementary Table S1). The access from the hallway to the laboratory is allowed by a pre-chamber (area about 20 m^2) connected to the same air conditioning system of the laboratory.

SiO_2 NPs are produced in a laboratory of area about 42.1 m^2 (Length = 6.8 m Width = 6.2 m and Height = 3.1 m) located at the ground floor of the Facility B (Figure 1(b)) equipped with mechanical ventilation (6 air change per hour) for air conditioning and windows for natural ventilation, in which also other types of NMs productions were made. PPE include coats, nitrile gloves, glasses (Supplementary Table S1). The access to the laboratory is inside the building, from the hallway.

Instrument locations in facilities A and B are also reported in Figure 1. In both cases workers worn personal devices (DM and Sioutas) with the probes placed in the PBZ and during the activities they move to the different workstations to perform each phase. The sample probes of other instruments (FMPS, NSAM, ELPI+, PAS2000, Sioutas and VOCs cartridge) were placed inside the laboratory ('NF' position). For the FLG case we placed DM, VOCs

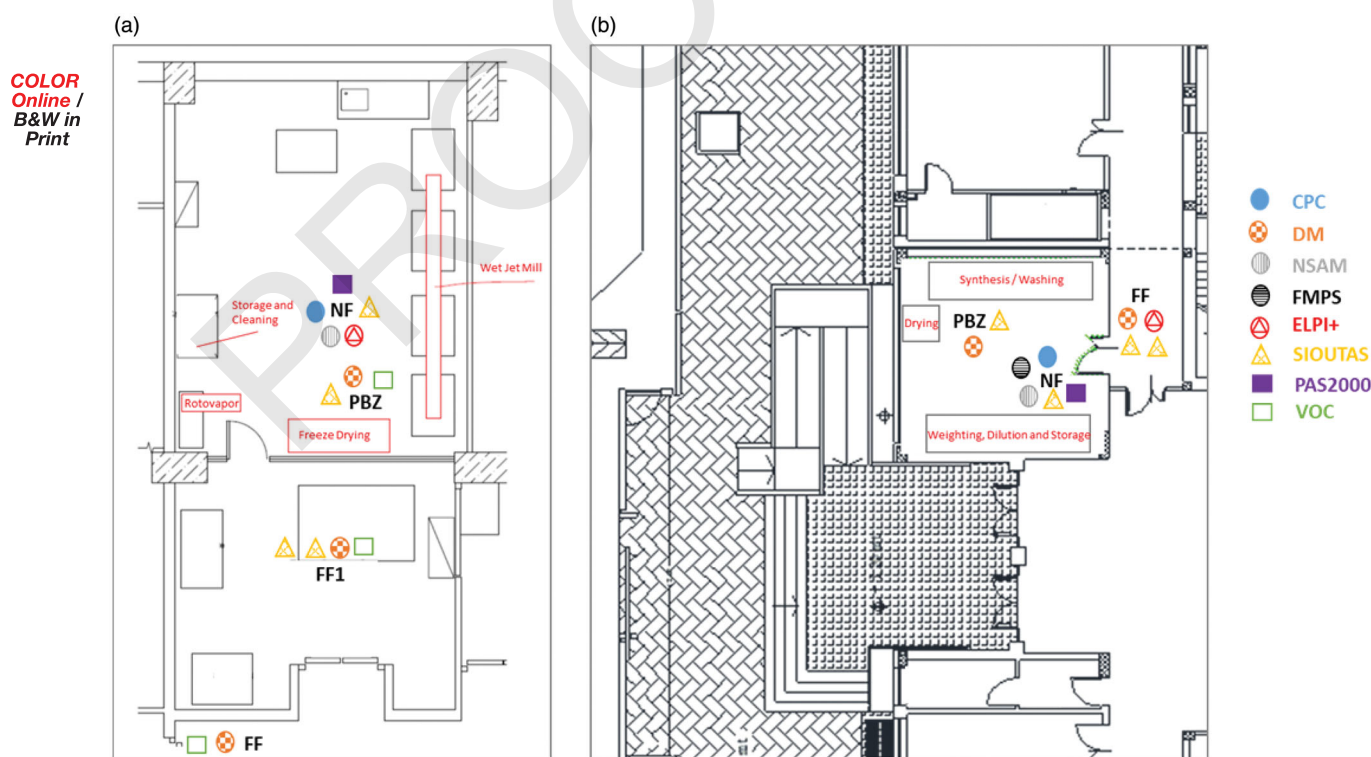


Figure 1. Instruments locations and sampling points in Facility A – FLG laboratory (a) and Facility B – SiO_2 NPs laboratory (b).

Table 2. Time schedules of measurement campaigns conducted for both case studies.

Day/hours	FLG process phase	Day/hours	SiO ₂ NPs process phase
Day 1 6:00PM–6:13PM	Instruments set up	Day 1 6:21PM–12:00PM	Instruments set up
6:16PM–6:21PM	A.3 freeze drying ^a (start)	Day 2 8:52AM–9:25AM	Instruments comparison #1
Day 2 9:20AM–9:40AM	Instruments comparison #1	9:45AM–10:06AM	Background ^b
10:00AM–10:12AM	Background ^b	10:06AM–10:24PM	B.1 Synthesis #1
10:12AM–5:35PM	A.2 Rotovapor	10:40AM–12:28AM	B.1 Synthesis #1
Day 3 10:05AM–5:50PM	A.1 Wet Jet Mill	7:40PM	B.3 Drying #1 (start)
Day 4 3:50PM–3:55PMM	A.3 Freeze Drying (stop)	Day 3 10:02AM–2:00PM	B.2 Washing
3:55PM–5:39PM	A.4 Storage and Cleaning	10:40AM–11:00AM	B.3 Drying #1 (stop + dryer opening)
Day 5 9:24AM–9:51AM	Instruments comparison #2	11:05AM	B.3 Drying #2 (start)
		2:25PM–2:38PM	B.4 Weighting Dilution and Storage #1
		3:00PM–3:20PM	B.3 Drying #2 (stop + dryer opening)
		4:05PM	B.3 – Drying #3 (start)
		Day 4 9:50AM–9:56AM	B.3 Drying #3 (stop + dryer opening)
		10:04AM–12:44PM	B.1 Synthesis #3
		11:57AM–12:00PM	B.4 Weighting Dilution and Storage #2
		12:47PM–12:50PM	B.4 Weighting Dilution and Storage #3
		1:11PM–3:45PM	B.3 Drying #4
		4:19PM–4:22PM	B.4 Weighting Dilution and Storage #4
		5:48PM	B.3 Drying #5 (start)
		Day 5 9:08AM–9:25AM	Instruments comparison #2
		10:01AM–10:04AM	B.3 Drying #5 (stop + dryer opening)

^aPhase A.3 runs during others activities for 50 hours until Day 4.

^bBefore the production activities.

cartridge and two Sioutas also in the pre-chamber ('FF1' position). In both cases we placed further instruments in the hallway ('FF' position), outside the laboratory near the access: VOCs cartridge and DM for FLG case; VOCs cartridge, ELPI+ and two Sioutas for SiO₂ NPs case.

Time schedules of two extensive sampling campaigns are reported in Table 2.

Workers involved in all production phases included in the sampling campaigns were also enrolled for the biomonitoring pilot study; subjects non-occupationally exposed to nanomaterials, working in the administrative offices, were selected as control group as reported in detail in the part II of the study (Ursini et al. 2020).

Instruments comparison

At the beginning and at the end of each measurement campaign instrument comparison sessions have been conducted at the same sampling point when no production activities were performed, in order to define the correlations among the instruments measuring the same parameter and to align the obtained values (Asbach et al. 2012). Such operation allowed us to compare measurement obtained by the devices placed in different

locations during the campaigns and to harmonize the instruments' response. In particular three DM have been compared to the CPC signal and the parameters of correlation lines ($CPC = \alpha DM + \beta$) for PNC have been obtained (Supplementary Tables S3–S5 and Figures S1–S3). Furthermore comparisons among three DM have been conducted to set instrument's diffusion (I_D) and filter (I_F) stage current signals according to Fierz et al. (2011) equations and to calculate D_{avg} and LDSA corrections (Supplementary Tables S4–S6 and Figures S2–S4). As reference instrument, the DM that better correlate to CPC values has been chosen. In the following text, the values corrected after the instrument comparison analysis will be identified by an asterisk.

Results

FLG case study

Real time measurements comparison between background and production

In Table 3 are summarized average values and standard deviations of background and process phases for all sampling positions: laboratory (NF), personal (PBZ), pre-chamber (FF1) and hallway (FF). Background line reports the measurements

Q2

Table 3. FLG background and production phases average values and standard deviations of PNC, D_{avg} and LDSA.

	NF (CPC)		PBZ (DM*)		FF1 (DM*)		FF (DM*)	
	Average	Standard deviation	Average	Standard deviation	Average	Standard deviation	Average	Standard deviation
PNC (part/cm ³)								
Background ^a	6,710	782	6,709	808	7,050	661	816	317
A.1 – Wet Jet Mill	2,885	511	2,185	560	n.a.	n.a.	470	216
A.2 – Rotovapor	6,114	3,420	5,682	3,151	5,506	2,509	816	317
A.4 – Storage and Cleaning	2,780	1,281	2,159	1,242	2,212	1,129	541	186
D_{avg} (nm)	NF (ELPI+)		PBZ (DM*)		FF1 (DM)		FF (DM*)	
	Avg.	St.Dev.	Avg.	St.Dev.	Avg.	St.Dev.	Avg.	St.Dev.
Background ^a	65.61	3.92	54.80	2.74	53.01	2.30	96.90	13.53
A.1 – Wet Jet Mill	89.33	6.45	78.21	10.29	n.a.	n.a.	125.15	17.65
A.2 – Rotovapor	70.62	11.30	55.55	8.28	56.65	9.45	96.90	13.53
A.4 – Storage and Cleaning	61.55	5.94	72.77	12.69	71.17	13.96	116.27	16.59
LDSA ($\mu\text{m}^2/\text{cm}^3$)	NF (NSAM)		PBZ (DM*)		FF1 (DM)		FF (DM*)	
	Avg.	St.Dev.	Avg.	St.Dev.	Avg.	St.Dev.	Avg.	St.Dev.
Background ^a	25.30	1.32	20.81	0.98	20.73	0.96	7.88	0.40
A.1 – Wet Jet Mill	13.80	1.49	11.93	0.99	n.a.	n.a.	7.94	0.79
A.2 – Rotovapor	19.89	7.83	16.95	5.60	15.60	5.30	7.88	0.40
A.4 – Storage and Cleaning	10.55	3.16	9.92	2.42	12.00	3.28	7.76	0.36

^aBefore the production activities.

conducted at the same locations, before the working activities. Missing values due to instrument failures are reported as not available (n.a.) in the table. D_{avg} values of ELPI+ are calculated in the size range 10–300 nm. Phase A.3 Freeze drying is conducted in parallel to the other phases A.1 Wet Jet Mill and A.2 Rotovapor, then the related values are not reported in the table.

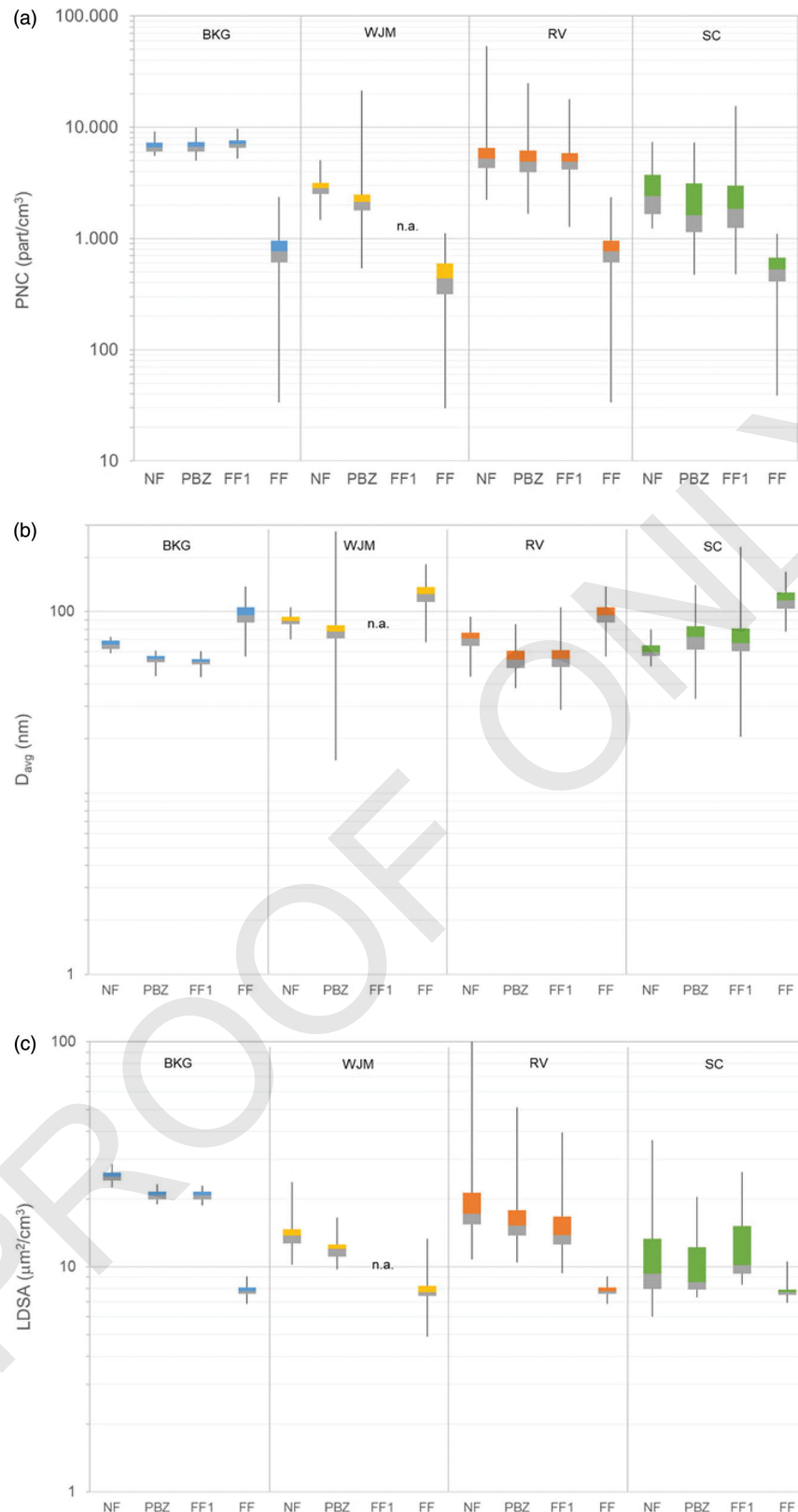
FF significant PNC value is 1,768 part/cm³; FF1 and NF significant values are respectively 9,032 and 9,057 part/cm³. NF background shows similar conditions to the FF1 also for of D_{avg} (65.61 nm and 53.01 nm respectively) and LDSA (25.30 $\mu\text{m}^2/\text{cm}^3$ and 20.73 $\mu\text{m}^2/\text{cm}^3$); NF average values are slightly higher than the PBZ ones probably due to the different position of sampling points and the different instrument used. Otherwise background FF is composed by few larger nano-objects with D_{avg} of 96.90 nm and corresponding LDSA of 7.88 $\mu\text{m}^2/\text{cm}^3$.

Distribution parameters of PNC, D_{avg} and LDSA for each production phase and background NF are represented by the boxplots in Figure 2. The whiskers indicate the minimum (lowest line) and the maximum (highest line) recorded value. The line inside the box represents the median value: the upper and the lower box-edges represent, respectively, the 75th and the 25th percentile. In general, by comparison of the median values, in the laboratory (NF) and in the pre-chamber (FF1), we note

some correspondence during all phases (albeit with slightly greatest intensity within the laboratory) confirming that the two internal rooms are subject to the same emission sources, both environmental and production related. Furthermore, the PNC PBZ values are always lower or equal to the NF ones.

During Wet Jet Mill phase (which for production needs was carried out in the day 3 after Rotovapor phase by starting a new process) the PNC and D_{avg} values are respectively lower and higher than the background NF values (Figure 2(a,b)) measured in the day before. The FF parameters in day 3 show the same trend, witnessing a generalized decrease in particulate levels and larger average dimensions compared to the day before, probably due to background environmental factors. During the Rotovapor phase the median values of the PNC measured in the three points (FF1, PBZ and NF) are slightly lower than those of the background NF albeit with greater variability and maximum values that widely exceed significant levels, with the laboratory values higher than the personal ones (Figure 2(a)). Same variation happened for LDSA (Figure 2(c)), while the corresponding D_{avg} values are slightly higher than those of the background NF (Figure 2(b)). During Storage and Cleaning phase in which the material is used in powder form, although the average values of the PNC always remain below the background NF values, there is a

COLOR
Online /
B&W in
Print



Q8 **Figure 2.** Box plots of PNC (a), D_{avg} (b) and LDSA (c) measured in each sampling point before the activities (BKG, light blue), phase A.1-Wet Jet Mill (WJM, yellow), phase A.2-Rotovapor (RV, orange) and phase A.4-Storage and Cleaning (SC, green) for FLG case study.

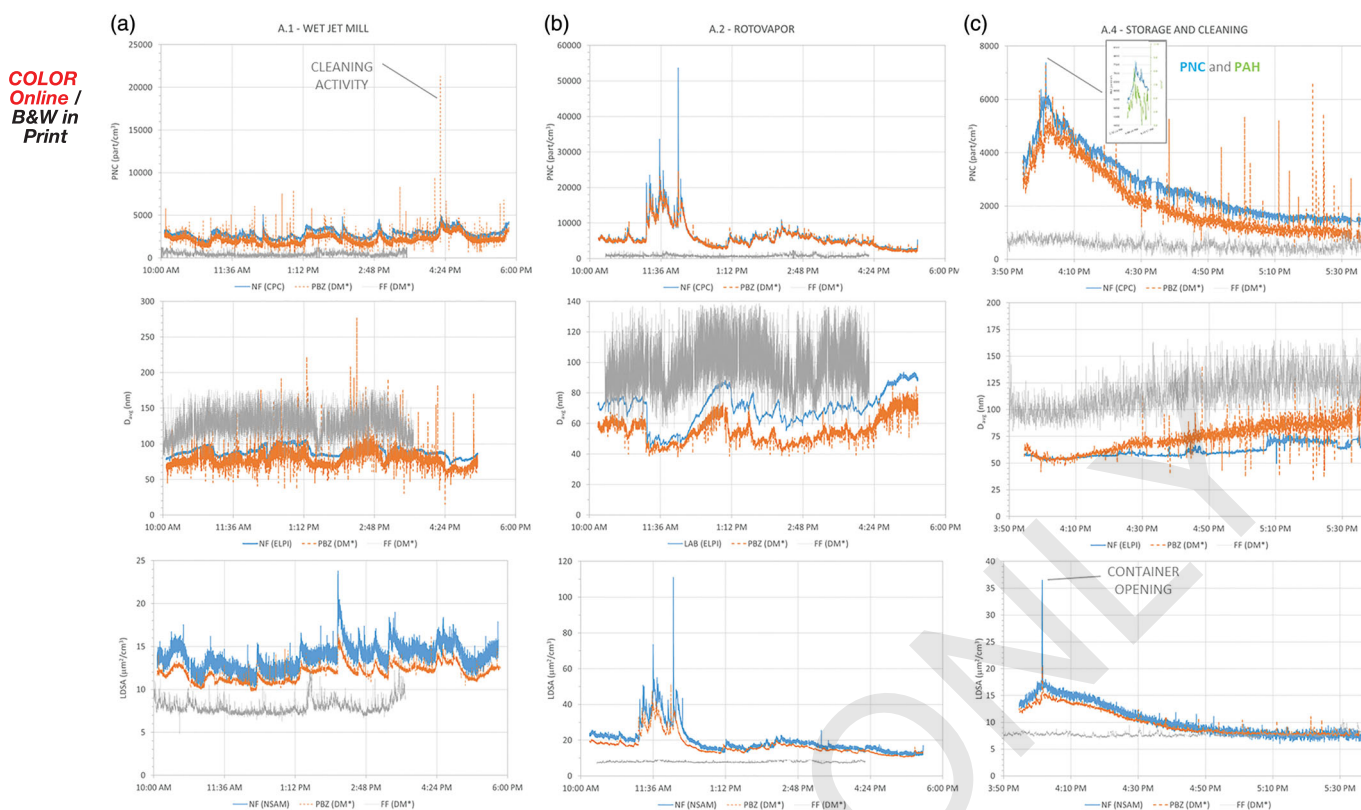


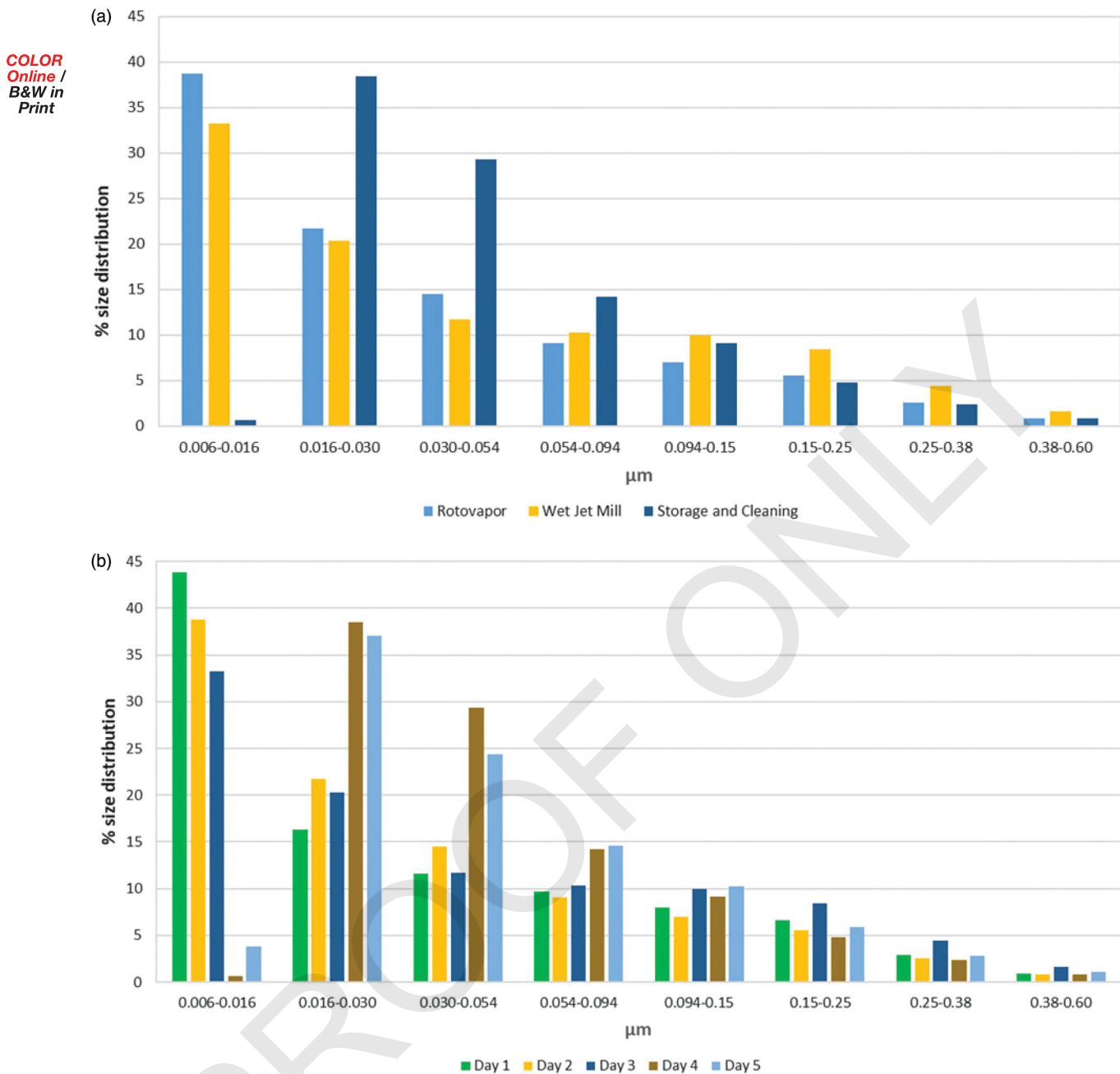
Figure 3. PNC, D_{avg} and LDSA time series for FLG process: A.1 Wet Jet Mill day 3 (a); A.2 Rotovapor day 2 (b); A.4 Storage and Cleaning day 4 (c).

greater variability of the signal (Figure 2(a)). Inside the laboratory the D_{avg} is slightly lower than the respective background NF while it stands on median value as 72.54 nm in the worker's PBZ (Figure 2(b)) higher than the PBZ background (54.88 nm). The LDSA is always lower than the background (Figure 2(c)).

The time series of the real-time parameters PNC, D_{avg} and LDSA are reported in Figure 3 for each monitored phase of the FLG production process, in order to highlight the behavior of the airborne nanoparticles in the PBZ compared to the levels found in the workplace (NF), taking advantage of the potential of high resolution measurements (1 Hz). During the Wet Jet Mill phase (Figure 3(a)) there is a generalized increase during the equipment cleaning operations from 4:15 PM onwards with a maximum peak detected in the PBZ of 21,000 part/cm^3 . In the Rotovapor phase (Figure 3(b)), on the other hand, the PNC peaks inside the laboratory also exceed 2–3 times the personal values. The trend of the PNC is in line with the LDSA while the D_{avg} is inverse: the increases in PNC correspond to decreases in the D_{avg} which

means that there is an introduction of small particles both in the laboratory and in the PBZ. During the Storage and Cleaning phase (Figure 3(c)) the trend of the PNC shows an increase when the operations start, followed by a decreasing trend associated to the lock of the internal air conditioning system (similar behavior both in the laboratory and in the PBZ). Furthermore, PNC peaks are detected by the personal device but not by the workplace monitor. There is a peak in LDSA ($37 \mu\text{m}^2/\text{cm}^3$) and PNC ($7,500 \text{ part}/\text{cm}^3$), with a corresponding decrease in D_{avg} up to 40 nm, between 3:55 PM and 4:00 PM in correspondence to the opening of the FLG container during the Storage and Cleaning phase. There was recorded also a photoelectric response by the PAS2000, as shown in the zoom of Figure 3(c); this signal is probably due to the soot present in the FLG container (see also PAH time series in Supplemental materials).

Figure 4 reports the normalized PSD of airborne nano-objects in the size range 6–600 nm measured by the ELPI+ in the NF position during each phase (Figure 4(a)) and by day (Figure 4(b)). The values related to each channel size are reported in



911
912
913
914
915
916
917
918
919
920
921

Figure 4. Particle size distribution (%) of airborne NMs measured by ELPI+ inside the FLG laboratory and normalized for the whole phase (a) and day (b).

percentage with respect to the total concentration obtained in the whole sampling period in order to highlight the contribution provided by the single particle size during the entire working phase. During the Storage and Cleaning phase about 90% of particles are in the size range 16–150 nm. PSD shows a peak value in the size range 16–30 nm with up to 67% of particles having dimensions between 16 nm and 54 nm (Figure 4(a)). Such distribution remains the same also in the following day morning (day 5 in Figure 4(b)). Otherwise, in the previous

922
923
924
925
926
927
928
929
930
931
932
933
934
935
936
937
938
939
940
941
942
943
944
945
946
947
948
949
950
951
952
953
954
955
956
957
958
959
960
961
962
963
964
965
966
967
968
969
970

days corresponding to the other two phases (day 2 Rotovapor and day 3 Wet Jet Mill) the size distribution looks like moved in the left side, with the majority of particles in the size range 6–30 nm.

Off-line analysis on airborne sampled materials

The mass concentrations of the particulate matter in the background and in the worker's PBZ (production) collected by the Sioutas impactors are reported in supplemental materials (Supplementary Figure S8). The devices had a sampling time of

COLOR
Online /
B&W in
Print

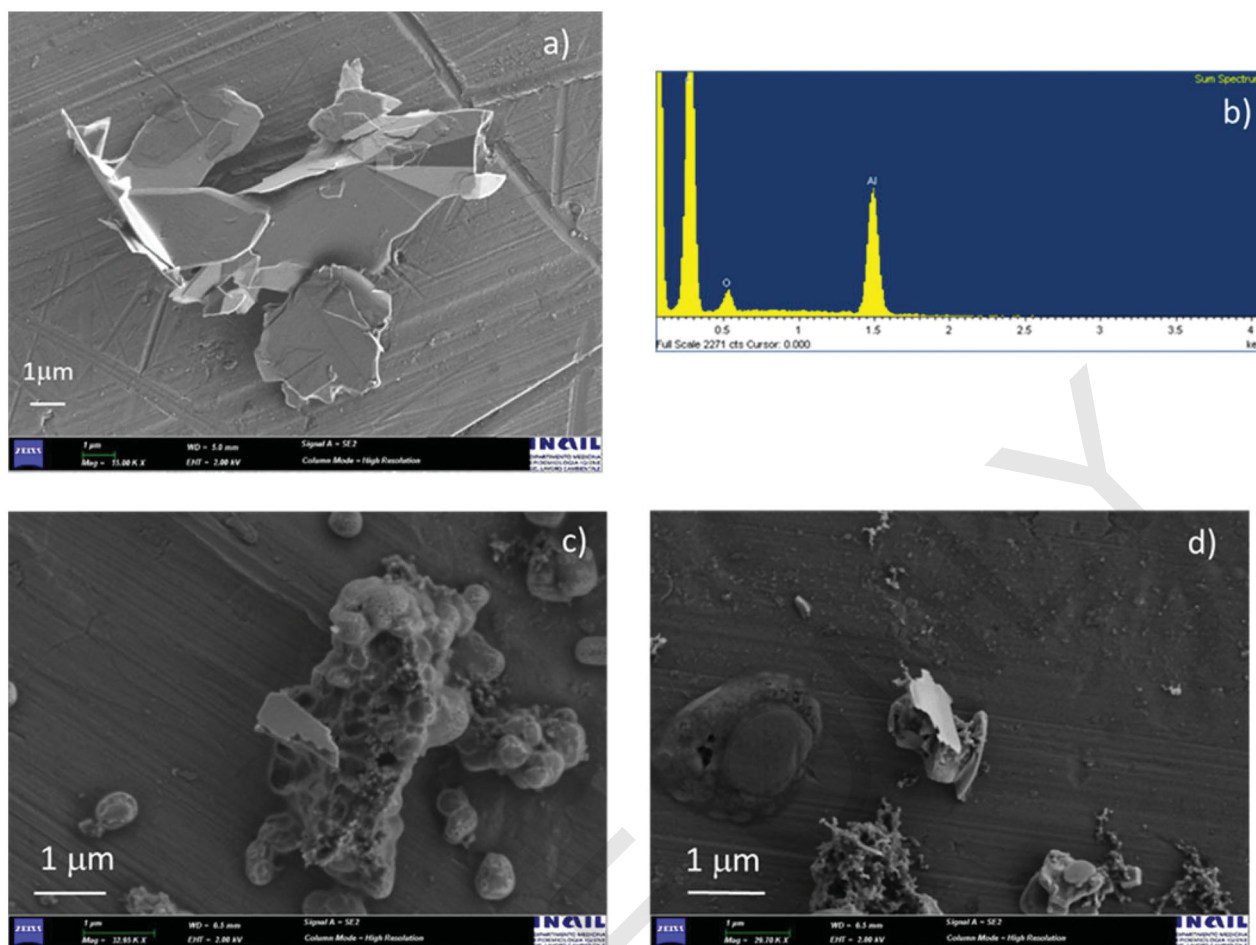


Figure 5. High-resolution SEM images and EDS spectra of FLG trial sample (a, b) and airborne sampled materials in the workplace (c, d).

1990 minutes (33.17 hours) each. Subtracting the background value from the production one with reference to the backup filter (BK), the concentration of particulate matter with aerodynamic diameter $<250\text{nm}$ ($\text{PM}_{0.25}$) to which the worker can be exposed in the operating conditions is up to $0.51\ \mu\text{g}/\text{m}^3$. Total particulate matter collected during the production inside the laboratory was $2.47\ \mu\text{g}/\text{m}^3$ (Supplementary Table S8).

Figure 5 shows the results of HR-SEM analysis: a trial sample of FLG, which is presented in the form of an aggregate with lateral dimensions in the range of few microns and consisting of smaller flakes is reported in Figure 5(a). The corresponding EDS spectrum (Figure 5(b)) confirms the clear prevalence of the signal of the carbon atoms compared to those of oxygen, as expected; aluminum (Al) signal comes from the Al substrate on which the FLG trial sample was deposited.

HR-SEM images in Figure 5(c,d) refer to the filters stages #8 (380–600 nm) and #10 (940–1,600 nm) of ELPI+, which sampled only during the Storage and Cleaning phase in day 4; they highlight structured layered material with clean and well-defined edges with lateral size lower than $1\ \mu\text{m}$ and similar to the morphology of the trial materials. It should be noted that these structures are placed on larger structures that seem to have acted as carriers. The fact that the structures in Figure 5(c,d) were not isolated but mixed with other sampled material of unknown origin, made the sample unstable so much that it was not possible to acquire EDS spectra having had to change the acquisition parameters with respect to the shown HR image.

SiO₂ NPs case study

Real time measurement comparison between background and production. As for the previous

Table 4. Background and production phases average values and standard deviations of PNC, D_{avg} and LDSA for SiO₂ NPs case study.

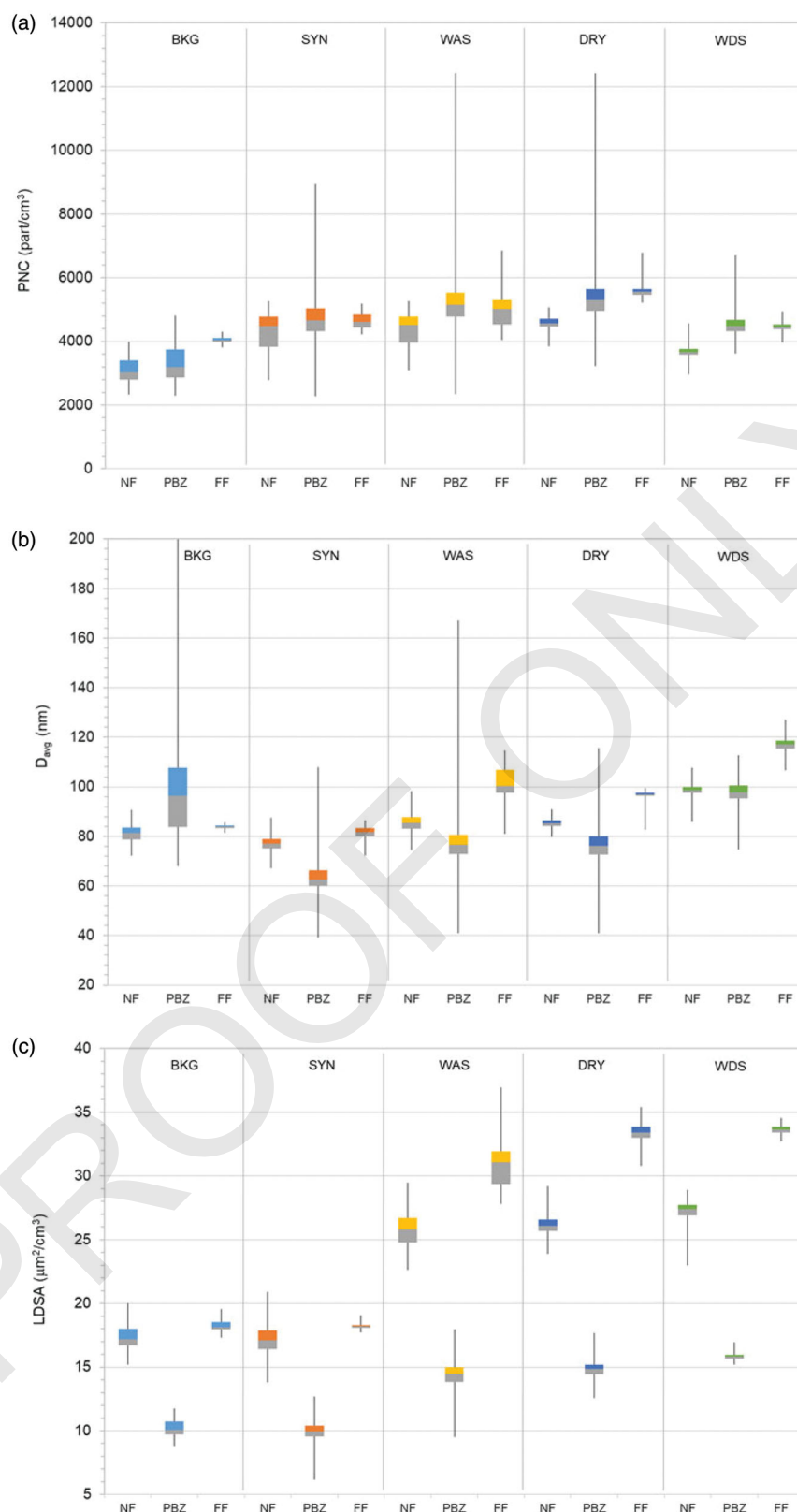
PNC (part/cm ³)	NF (CPC)		PBZ (DM*)		FF (ELPI+)	
	Avg.	St.Dev.	Avg.	St.Dev.	Avg.	St.Dev.
Background ^a	3,095	361	3,296	540	4,051	82
B.1 – Synthesis	4,280	597	4,693	579	4,638	220
B.2 – Washing	3,947	465	5,144	644	4,957	455
B.3 – Drying	4,571	193	5,312	592	5,563	141
B.4 – Weighting Dilution and Storage	3,745	289	4,532	308	4,451	128
D_{avg} (nm)	NF (FMPS)		PBZ (DM*)		FF (ELPI+)	
	Avg.	St.Dev.	Avg.	St.Dev.	Avg.	St.Dev.
Background ^a	81.16	3.29	97.46	16.94	83.80	0.75
B.1 – Synthesis	77.07	2.63	74.96	6.38	81.37	2.45
B.2 – Washing	91.11	3.28	77.23	7.12	101.67	5.48
B.3 – Drying	85.34	1.67	76.65	6.31	96.88	1.18
B.4 – Weighting Dilution and Storage	98.66	2.22	97.83	4.45	117.06	2.48
LDSA ($\mu\text{m}^2/\text{cm}^3$)	NF (NSAM)		PBZ (DM*)		FF (ELPI+)	
	Avg.	St.Dev.	Avg.	St.Dev.	Avg.	St.Dev.
Background ^a	17.30	0.86	10.19	0.63	18.23	0.42
B.1 – Synthesis	17.19	1.11	10.30	0.35	20.36	1.30
B.2 – Washing	25.36	1.19	14.33	0.94	30.84	1.68
B.3 – Drying	26.16	0.69	14.81	0.60	33.45	0.65
B.4 – Weighting Dilution and Storage	27.32	0.65	15.81	0.21	33.58	0.30

^aBefore the production activities.

case study, we summarized in Table 4 the background and process phases average values and standard deviations for all monitoring positions: laboratory (NF), personal (PBZ) and hallway (FF). FF PNC and LDSA values are calculated from ELPI response in the size range 10–1000nm, while D_{avg} values are reported for the size range 10–300 nm in order to obtain a better comparison among all the instrument values. For B.3 phase (Drying) we report here the values related to the dryer opening activities in which the worker extracts the SiO₂ NPs in powder form. PNC lowest values are measured before the production in all the positions (background NF, PBZ and FF). During all phases of the process the average values of the real-time FF PNC measurements in the fraction considered (10–1000nm) are higher than those NF; in the worker's PBZ there is a higher value than the FF during the Synthesis, Washing and Weighting Dilution and Storage phases. However, the D_{avg} of the particles (10–300nm) is always lower within the laboratory (with PBZ values lower than the NF ones during all phases) compared to the FF. On the other hand, LDSA (10–1000nm) is always higher FF than inside the laboratory (both NF and PBZ).

Distribution parameters of PNC, D_{avg} and LDSA for each production phase and background NF are represented by the boxplots in Figure 6. We noted higher values of PNC during all the production phases compared to the background (Figure 6(a)) with great variability of personal measurements. PBZ D_{avg} values are lower than the background ones, with minimum values reaching 40 nm in the Synthesis, Washing and Drying phases (Figure 6(b)). The LDSA highest values measured by the DM in the range 10–300 nm are related to the Weighting, Dilution and Storage compared to the respective background ones (Figure 6(c)).

Figure 7 reports the time series of SiO₂ NPs production process, showing that the PNC levels of personal exposure (PBZ) are always higher than those recorded in the laboratory (NF) in all phases of the process (with the exception of a small part of the synthesis in Figure 7(a)). Furthermore, personal values show greater variability. In particular, during the dryer opening we highlight a concentration peak at 10:41AM higher than 12,000 part/cm³, corresponding to a decrease in the average diameter up to 40 nm (Figure 7(b)). LDSA time series confirm at the same time the peak value of 17.68 $\mu\text{m}^2/\text{cm}^3$ (Figure 7(c)).



Q9 Figure 6. Box plots of PNC (a), D_{avg} (b) and LDSA (c) measured in each sampling point before the activities (BKG, light blue), phase B.1-Synthesis (SYN, orange), phase B.2-Washing (WAS, yellow), phase B.3-Drying (DRY, blue) and phase B.4-Weighting Dilution and Storage (WDS, green) for SiO₂ NPs case study.

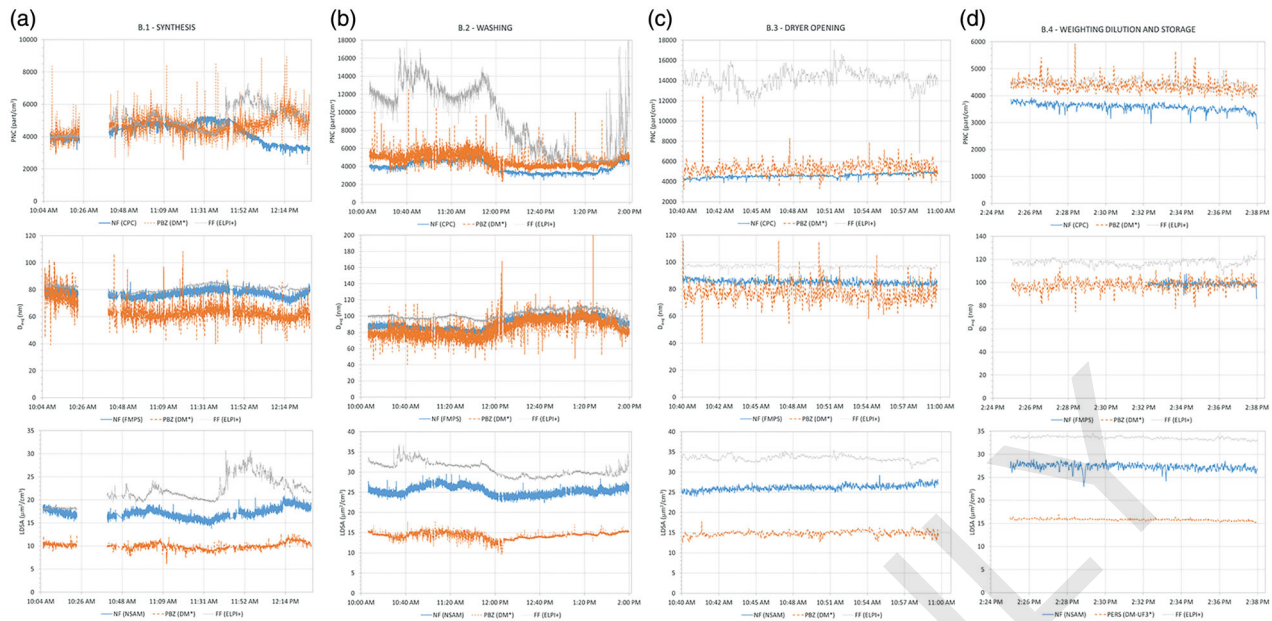


Figure 7. PNC, D_{avg} and LDSA time series for SiO_2 NPs process: B.1 Synthesis (a); B.2 Washing (b); B.3 Drier opening (c), B.4 Weighting Dilution and Storage (d).

Figure 8 reports the normalized PSD (in percentage) of airborne nano-objects in the size range 6–600 nm measured NF by FMPS (Figure 8(a)) and FF by ELPI+ (Figure 8(b)) during each phase. Production phases are characterized by a size distribution with the majority of particles in the size range 30–154 nm. The NF background before the production show a size distribution moved in the right side (Figure 8(a)). FF is always composed by small nanoparticles (6–16 nm) for the great majority of the size distribution (Figure 8(b)).

Off-line analysis on airborne sampled materials.

Mass concentrations of the particulate matter collected by two Sioutas samplers in the background and in the worker's PBZ (production) are reported in supplemental materials (Supplementary Figure S9). The instruments had a total sampling time of 2123 minutes (35.38 hours) in the production and 2101 minutes (35.02 hours) in the background respectively. Subtracting the background value from the production, with reference to the backup filter (BK), the concentration of $\text{PM}_{0.25}$ to which the worker can be exposed in the operating conditions was up to $2.78 \mu\text{g}/\text{m}^3$. Total particulate matter related to the production was $3.25 \mu\text{g}/\text{m}^3$ (Supplementary Table S9).

HR-SEM morphological analysis of the sampled filters revealed rare silica particles similar in size and

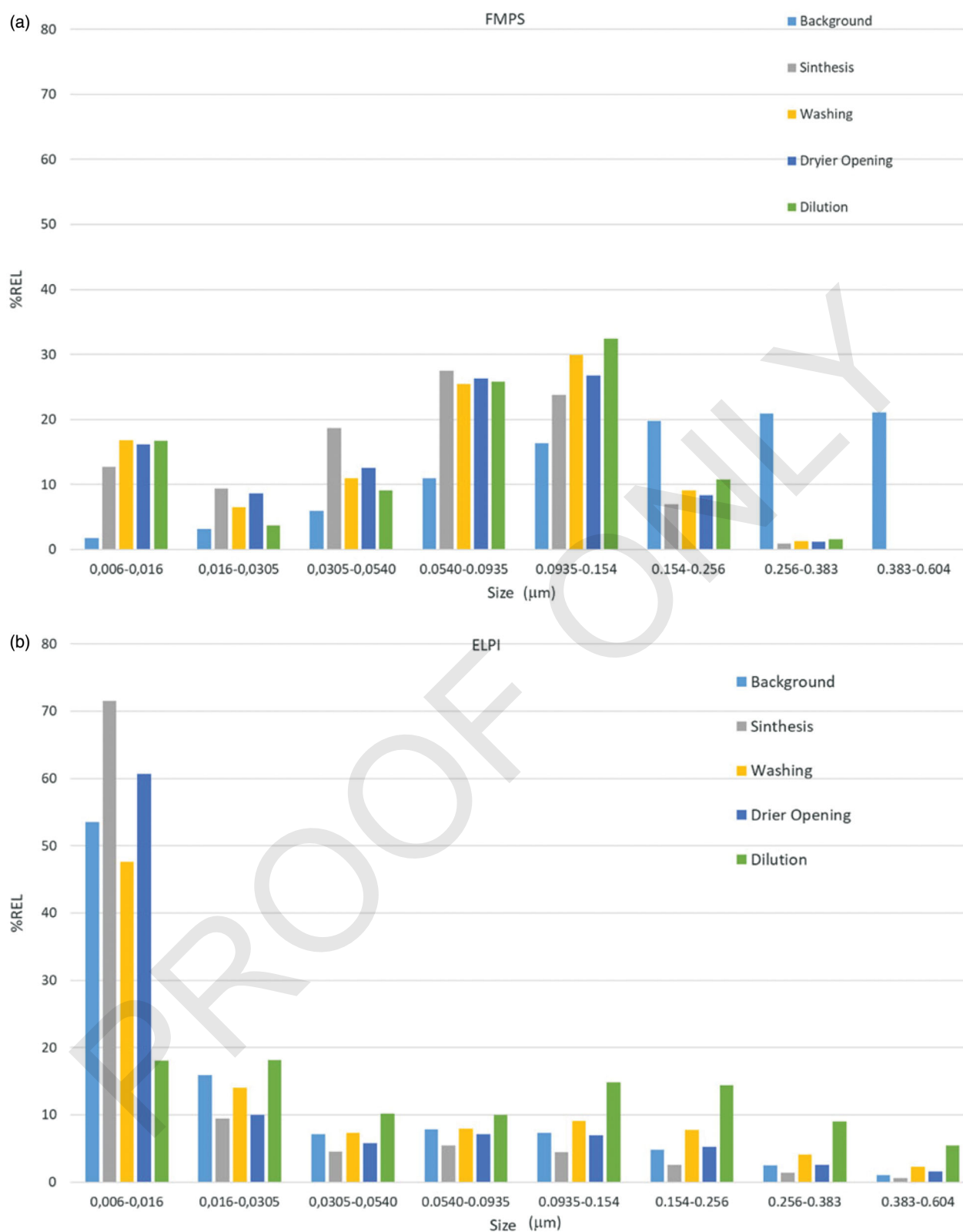
shape to the produced SiO_2 NPs. Figure 9(a) shows HR-SEM images of the SiO_2 NPs of the trial sample forming a star-shaped aggregate and Figure 9(b) shows the sampled filter collecting particles in the range 250–500 nm in which an aggregate, measuring a few hundred nanometers in its main length, is made up of spherical particles that have dimensions comparable with those of the trial sample.

A magnified area of Figure 9(b) is reported in panel c, in which two different areas have been indicated by one or two asterisks to indicate the EDS acquisition zones (Figure 9(d**), e*). In the EDS spectrum of Figure 9(e)* the signal contribution of Si atoms is well evident; it is indeed completely absent in the EDS background spectrum (Figure 9(d)**), that highlights the shape and the typical elemental composition in a region where the EDS signal is only acquired from the Al substrate and not from the particles.

Discussion

FLG case study

The real-time values measured at high resolution (1 Hz) of PNC, D_{avg} and LDSA showed an overall different exposure scenario inside the laboratory (NF) and in the worker's PBZ during all production phases, compared to the FF values. The PNC levels were on average 1–3 times higher than the



1407
1408
1409
1410
1411
1412
1413
1414
1415
1416
1417
1418
1419
1420
1421
1422
1423
1424
1425
1426
1427
1428
1429
1430
1431
1432
1433
1434
1435
1436
1437
1438
1439
1440
1441
1442
1443
1444
1445
1446
1447
1448
1449

Figure 8. Particle size distribution (%) of airborne NMs for SiO₂ NPs case normalized for the whole measurement period by phase inside the laboratory (a) and in the hallway (b). Background values are measured before the activities.

1450
1451
1452
1453
1454
1455

significant FF value, but always lower than NF and PBZ background levels (near to 9,000 part/cm³). Furthermore the FF PNC values (in the range

10–1000nm) measured in parallel in the hallway in all the days of production are almost constant (around 800–1,000 part/cm³ with low standard

COLOR
Online /
B&W in
Print

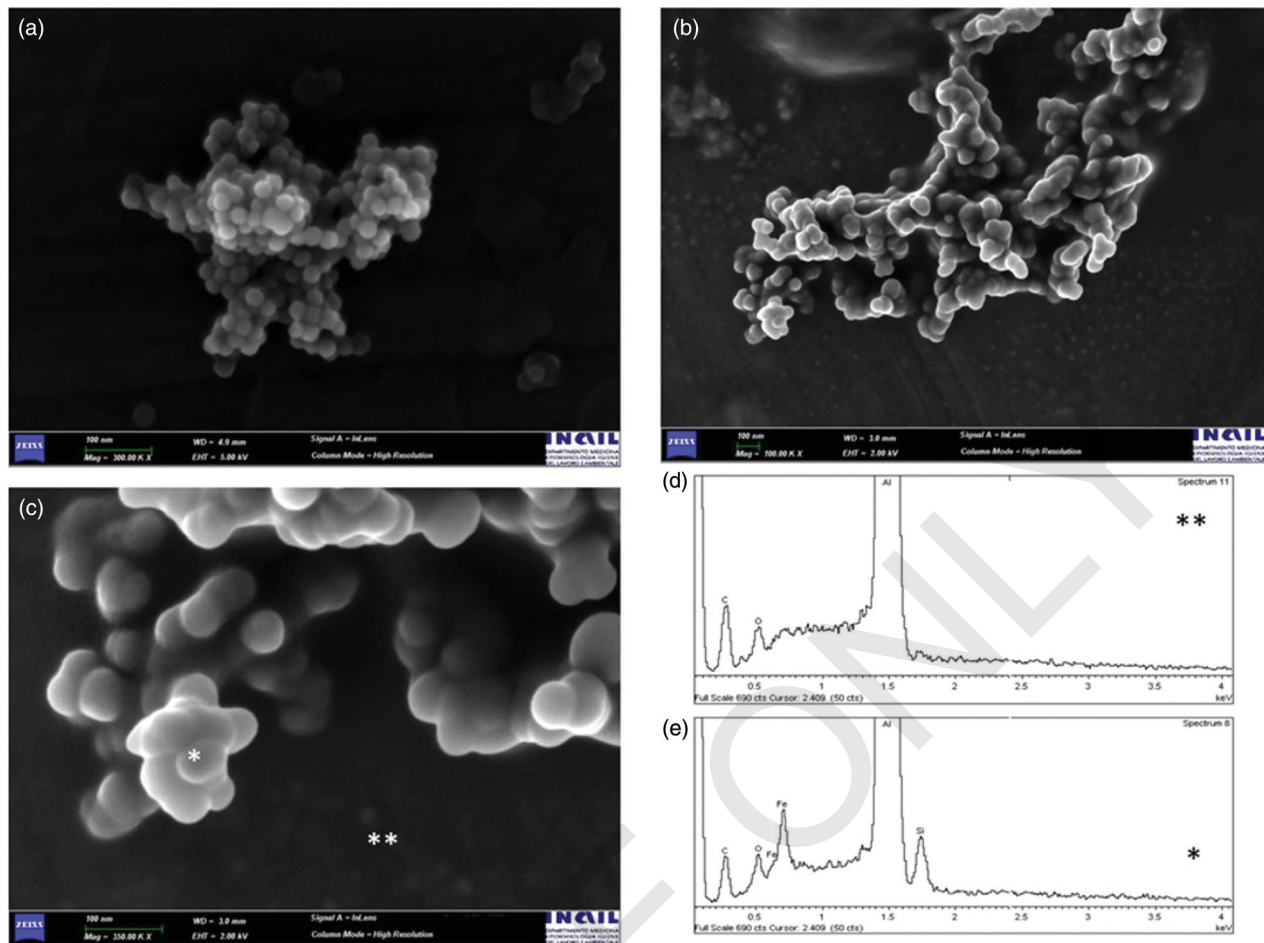


Figure 9. High resolution SEM images of SiO₂ NPs trial sample (a) and airborne sampled materials in the worker's PBZ (b, c). EDS spectra acquired on two areas of the sampled filter (c) are labeled by one or two asterisks (d**, e*).

deviation) and lower than the values recorded both in the pre-chamber (FF1) and inside the laboratory (NF and PBZ). LDSA showed the same trend. The diffusion charging D_{avg} of the particles during the production remained always below the FF values. D_{avg} in the hallway is around 100 nm in day 2 of activity (Background NF and Rotovapor) and grows up to 120–130 nm in the following days (Wet Jet Mill and Storage and Cleaning). Vice versa, both inside the laboratory and in the pre-chamber, the average values are always lower: around 60 nm in the background NF and in the Rotovapor phase and 70–75 nm during Wet Jet Mill and Storage and Cleaning. This behavior is probably due on one hand to the different volume, ventilation and crowding conditions between the hallway (FF) and the two internal rooms (NF, PBZ and FF1); on the other hand it is related to the activities that take place inside the laboratory to which the emission of nano-particulate matter may be associated.

Therefore, taking as a reference FF value, all the activities carried out during FLG production may be at potential risk of NMs (but not necessarily of FLG) emission. However, in order to make consideration on the PNC values associated to the real exposure scenario inside the laboratory, the NF background may be the reference as significant value (9,057 part/cm³). This is the highest value of recorded background then it could represent the worst case exposure scenario. PNC levels are lower than such significant values during the Wet Jet Mill and Storage and Cleaning phases; on the contrary, they far exceed the significant values during the Rotovapor phase. The previous data, associated with the general decrease in PNC on days 3 and 4, confirm a change in the characteristics of the background particulate in these two days compared to day 2. The same type of variation is present in the pre-chamber (FF1) and inside the laboratory (NF and PBZ) during the production phases. This

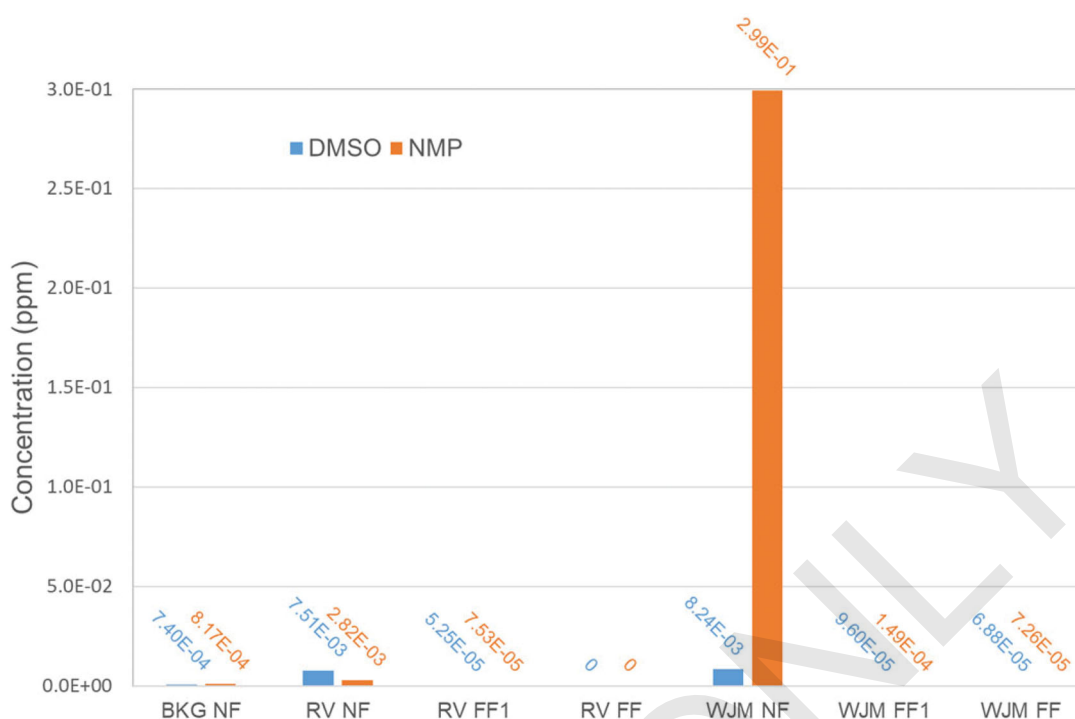


Figure 10. GC-MS analysis of solvents DMSO and NMP concentration (ppm) in the workplace (NF) during Rotovapor (RV) and Wet Jet Mill (WJM) phases compared to the values before the activities in the same position (BKG NF) and to the values during the activities in the hallway (FF) and in the pre-chamber (FF1).

situation is also confirmed by PAHs time series measured by PAS2000 as reported in [Supplementary Table S7](#) and [Figures S5–S7](#). During day 3 PAH concentration had an average value of 5.64 ng/cm^3 (dev.st. 3.94) while on day 4 the mean value rises to 11.12 ng/cm^3 showing high variability during the day (dev.st. 10.61). This growth of PAHs can be associated with an external contribution (e.g. through the ventilation system), in fact the average PAHs concentration on day 4 from 3:55 PM (during Storage and Cleaning phase by the end of the day) when the intake of air from the laboratory air conditioning system was turned off, drops to 5.13 ng/cm^3 (dev.st. 0.85).

During the Wet Jet Mill and Rotovapor phases, the peaks of PNC and LDSA corresponding to the simultaneous decrease in D_{avg} , could be linked to the use of solvents such as DMSO, NMP (and others), in any case with values always below the reference occupational exposure limits. During the Wet Jet Mill phase ([Figure 3\(a\)](#)) there is a generalized increase during the equipment cleaning operations. These intensity variations are also connected to the use of DMSO and NMP solvents during all the process by the workers wearing the DM probe, plus Isopropyl alcohol and acetone for cleaning the

beakers. This is confirmed, by VOCs analysis carried out by GC-MS ([Figure 10](#)) that in the Wet Jet Mill phase shows the presence of NMP (2.99×10^{-1} ppm) in greater quantity than the DMSO (8.24×10^{-3} ppm). The mass concentration (ppm) values of these solvents are in any case below the occupational exposure limit values available in the literature: 50 ppm for DMSO (ILO 2000) and 10 ppm for NMP (ILO 2014) respectively. The extreme ease of aggregation of the solvents with airborne particles would have led to the formation of the so-called secondary organic aerosol, thus causing a corresponding lowering of the PNC with an increase in the D_{avg} (Kim et al. 2015). Also in the Rotovapor phase, the increases in PNC could be associated with the use of solvents (in particular DMSO which replaces the NMP during the Rotovapor washing) which are not present in the background of the laboratory (NF), in the pre-chamber (FF1) and in the hallway (FF).

The analysis of contribution of different particle size to the total PSD ([Figure 4](#)) allowed us to compare process phases and production days. The phase at higher risk of potential exposure to NMs resulted the Storage and Cleaning phase (day 4), in which the material is handled in powder form, and a change in the size distribution within the

laboratory occurred: 90% of particles were in the size range 16–150 nm, greater than in the previous days when the majority of the particles were in a lower size range. We highlighted the PAH signal associated to the soot present in the FLG container during its opening at the beginning of Storage and Cleaning phase and we can assume that the emitted particles included FLG, according also to the findings reported by Yeganeh et al. (2008) for carbon-based NMs emission. Furthermore, HR-SEM EDS analyses of the filters sampled during Storage and Cleaning phase showed rare particles attributable in size and shape to those produced, but often linked to larger and visible structures in various overlapping layers. Despite the morphology and the dimensions of airborne materials refer to the material as it is (Figure 5(a,b)), it would be appropriate to deepen this characterization using analytical techniques such as, for example, Raman spectroscopy or the Selected Area Electron Diffraction (SAED) with TEM, which are functional to put highlights the characteristic parameters of the honeycomb lattice structure of graphene (Tombolini et al. 2020).

SiO₂ NPs case study

Q3 From the comparison between the background NF significant values and average PNC values during the production (Table 5), the phases in which a possible emission of NPs has been highlighted are: phase B.1 Synthesis and phase B.3 Drying (when the freeze dryer is opened).

The real-time time series measurements (Figure 7) in the operator's PBZ showed PNC and LDSA levels higher than the laboratory sampling point during all the production phases, with a decrease of the D_{avg} . In particular a PNC peak of about three times the significant value is recorded in the Drying phase when the freeze dryer is opened, associated with a rapid decrease in D_{avg} up to about 40 nm. The decrease of average diameter of airborne particles corresponding to a simultaneous increase of PNC, may refer to an emission of small nanoparticles during this process phases. D_{avg} personal values are closing to the size of the produced SiO₂ NPs (50 nm) also during Synthesis and Washing phases. The personal LDSA values recorded by the DM are always lower than those measured by the NSAM inside the laboratory although they maintain

the same trend; this is probably due to the different position of two sampling probes but also to the different dimensional range of the two instruments, which for NSAM includes also particles up to 1000 nm.

The PSD analysis confirms the potential emission during the production. All phases show a different size distribution inside the laboratory compared both to the background NF and to the background FF measured in parallel in the hallway: here almost all the particles were in the range 6–16 nm showing a clear influence by external contributions (Figure 8(b)). During all the production phases inside the laboratory the percentage of particles in this range is lower; on the contrary particles from 30 to 154 nm, which include the typical size of produced SiO₂ NPs, were 2–3 times higher in the laboratory than the FF values.

Finally, the morphological and elemental analysis by HR-SEM EDS of the filters sampled in the worker's PBZ (Figure 9) confirmed the presence of rare SiO₂ particles similar in size and shape to the produced NPs and their agglomerated structures.

In this case the mass concentration of PM_{0.25} in the worker's PBZ was up to 2.78 µg/m³. This value may be intended as the upper limit of the mass of nanomaterials with aerodynamic diameter <250 nm to which the worker is potentially exposed during the production process. This value corresponds to 85% of total particulate matter collected during the SiO₂ NPs production subtracted by the background. It was higher than the FLG case, in which the PM_{0.25} represents only 21% of total particulate matter collected in the operating conditions of the study.

Such experimental values are under the official limit value for bulk silica materials calculated by Murugadoss et al. (2017) and were recently correlated with the doses tested in a 3-D in vitro platform by Di Cristo et al. (2020). Such in vitro system was developed to provide regulatory-oriented toxicological data for risk classification of nanomaterials.

Conclusions

In the present study, two exposure measurement campaigns were conducted in different production sites of FLG (facility A) and SiO₂ NPs (facility B),

according to the harmonized strategies by OECD and WHO, based on tiered levels of investigation. This approach integrates real-time devices and time-integrated samplers for the following off-line chemical and morphological analysis, in order to identify the contribution of production compared to the background and personal exposure compared to the workplace. From the evidences of the conducted study, the presence of airborne FLG produced in the facility A cannot be excluded, although the analysis of the materials sampled in workplace air and in the worker's PBZ require further insights necessary for the identification of the typical honeycomb structure of graphene. On the contrary, the presence of airborne SiO₂ NPs during production at the facility B seems to be confirmed both by real-time data and chemical-morphological analysis. The results of this study have been integrated with the evidences of biomonitoring as reported by Ursini et al. (2020) in the part II of the same research. The biomonitoring pilot study used sensitive biomarkers of cyto-genotoxicity and oxidative DNA damage (Micronucleus Cytome assay on buccal cells and Fpg-comet assay on blood), biomarkers of oxidative stress on Exhaled Breath Condensate and of inflammation (cytokine release) on blood. The study, demonstrates that buccal Micronucleus Cytome assay and Fpg-comet assay are the most sensitive biomarkers of early, still repairable, genotoxic and oxidative effects. In particular, the Buccal Micronucleus Cytome assay showed an increase, although not statistically significant, of micronucleus (MN) frequency in respect with controls for both groups of workers (FLG and SiO₂ NPs). Moreover, taking into account the MN positive subjects (with MN frequency higher than a cutoff value), higher percentages of MN positive subjects in both the worker groups in respect with controls were found. Fpg-comet assay results showed the highest direct DNA damage in the group of SiO₂ NPs workers; finally the oxidative DNA damage in terms of subjects positive (with oxidative DNA damage higher than a cutoff value), was higher in FLG workers either in respect to controls or in respect to SiO₂ NPs workers.

Under these conditions and until the assessments toward the quantification of workers exposure will be deepened, also in a comprehensive analysis integrated with the evidences of the biomonitoring

study, it was useful to recommend some risk management measures, to be strengthened in both facilities to mitigate the potential risk for the workers involved in the processes. Such measures, within the risk management hierarchy, should primarily include the possibility to contain the phases at higher risk through the implementation of structural and equipment interventions aimed at reducing the interface between the operator and the handled materials (e.g. closed systems, glove boxes, ventilated boxes). Furthermore it will be possible to organize of the processes with a view to reducing working times (e.g. implementation of specific procedures and shifts). Finally we recommend to enforce the maintenance programs in order to guarantee the efficiency of collective (e.g. aspiration hoods) and personal (e.g. gloves, glasses, masks and safety clothing) protective equipment: PPE should be worn by the workers during their presence in the production laboratories in all the phases in which the risk of contact with the material in powder form may happen as from the evidences of the present study.

In conclusion, based on the evidences of the present study, the re-design of production processes through a prevention-through-design approach, may represent an added value that will integrate the workers' health and safety needs with the production requirements, in the view to achieve more responsible and sustainable technological innovation processes.

Acknowledgments

The authors are grateful to Dr. Mariada Malvindi, Dr. Elisa Mantero and Dr. Luigi Marasco from Italian Institute of Technology, Italy for their expert collaboration in the case studies.

Disclosure statement

The authors declare no conflict of interest.

Funding

The present study is part of the Project 'Nano and Key enabling technologies within the innovation processes: risk and opportunities in occupational settings by prevention through design (NanoKey),' funded by the Italian Workers' Compensation Authority (INAIL) and coordinated in cooperation between the INAIL Department of Occupational and

Environmental Medicine Epidemiology and Hygiene, and the Italian Institute of Technology (IIT). The findings and conclusions in this publication are those of the authors and do not necessarily represent the views of the employing organizations.

References

Asbach, C., H. Kaminski, D. von Barany, T. A. Kuhlbusch, C. Monz, N. Dziurawitz, J. Pelzer, et al. 2012. "Comparability of Portable Nanoparticle Exposure Monitors." *The Annals of Occupational Hygiene* 56 (5): 606–621. doi:10.1093/annhyg/mes033.

Bergamaschi, E., F. Murphy, C. A. Poland, M. Mullins, A. L. Costa, E. McAlea, L. Tran, et al. 2015. "Impact and Effectiveness of Risk Mitigation Strategies on the Insurability of Nanomaterial Production: Evidences from Industrial Case Studies." *Wiley Interdisciplinary Reviews. Nanomedicine and Nanobiotechnology* 7 (6): 839–855. doi:10.1002/wnan.1340

Boccuni, F., R. Ferrante, F. Tombolini, D. Lega, A. Antonini, A. Alvino, P. Pingue, et al. 2018. "Workers' Exposure to Nano-Objects with Different Dimensionalities in R&D Laboratories: Measurement Strategy and Field Studies." *International Journal of Molecular Sciences* 19 (2): 349. doi:10.3390/19020349.

Brouwer, D., R. Boessen, B. van Duuren-Stuurman, D. Bard, C. Moehlmann, C. Bekker, W. Fransman, et al. 2016. "Evaluation of Decision Rules in a Tiered Assessment of Inhalation Exposure to Nanomaterials." *The Annals of Occupational Hygiene* 60 (8): 949–959. doi:10.1093/annhyg/mew045

Bukowiecki, N., D. B. Kittelson, W. F. Watts, H. Burtscher, E. Weingartner, and U. Baltensperger. 2002. "Real-Time Characterization of Ultrafine and Accumulation Mode Particles in Ambient Combustion Aerosols." *Journal of Aerosol Science* 33 (8): 1139–1154. doi:10.1016/S0021-8502(02)00063-0.

Del Rio Castillo, A. E., V. Pellegrini, A. Ansaldo, F. Ricciardella, H. Suna, L. Marasco, J. Buha, et al. 2016. "High-yield production of 2D crystals by wet-jet milling, in: Technology". Patent no. PCT/IB2016/057108

Di Cristo, L., F. Boccuni, S. Iavicoli, and S. Sabella. 2020. "A Human-Relevant 3D In Vitro Platform for an Effective and Rapid Simulation of Workplace Exposure to Nanoparticles: Silica Nanoparticles as Case Study." *Nanomaterials* 10 (9): 1761. doi:10.3390/nano10091761.

European Committee for Standardization (CEN). 2012. "Workplace Exposure – General Requirements for the Performance of Procedures for the Measurement of Chemical Agents". EN 482:2012 + A1:2015.

Evans, D. E., B. K. Ku, M. E. Birch, and K. H. Dunn. 2010. "Aerosol Monitoring During Carbon Nanofiber Production: Mobile Direct-Reading Sampling." *The Annals of Occupational Hygiene* 54 (5): 514–531. doi:10.1093/annhyg/meq015

Fadeel, B., C. Bussy, S. Merino, E. Vazquez, E. Flahaut, F. Mouchet, L. Evariste, et al. 2018. "Safety Assessment of Graphene-Based Materials: Focus on Human Health and the Environment." *ACS Nano* 12 (11): 10582–10620. doi:10.1021/acsnano.8b04758

Ferrante, R., F. Boccuni, F. Tombolini, S. Iavicoli. 2019. "Measurement Techniques of Exposure to Nanomaterials in Workplaces." In *Nanotechnology in Eco-Efficient Construction*, edited by Pacheco Torgal, 785–813. 2nd ed. Elsevier.

Fierz, M., C. Houle, P. Steigmeier, and H. Burtscher. 2011. "Design, Calibration, and Field Performance of a Miniature Diffusion Size Classifier." *Aerosol Science and Technology* 45 (1): 1–10. doi:10.1080/02786826.2010.516283.

Hubbs, A., D. W. Porter, V. Castranova, L. Sargent, and K. Sriram. 2013. "Nanoparticulates." In *Haschek and Rousseaux's Handbook of Toxicologic Pathology*, edited by Wanda M. Haschek, Colin G. Rousseaux and Matthew A. Wallig, 1373–1419. 3rd ed. London, UK: Academic Press.

International Commission on Radiological Protection (ICRP). 1994. "Human Respiratory Tract Model for Radiological Protection." In *ICRP Publication No. 66. Annals of the ICRP*, edited by H Smith. Tarrytown, NY: Pergamon Press.

International Labour Organization (ILO). 2000. "Dimetil Sulfoxide." ICSC: 0459, April 2000.

International Labour Organization (ILO). 2014. "N-Metil-2-Pirrolidone." ICSC: 0513, April 2014.

Jeelani, P. G., P. Mulay, R. Venkat, and C. Ramalingam. 2020. "Multifaceted Application of Silica Nanoparticles. A Review." *Silicon* 12 (6): 1337–1354. doi:10.1007/s633-019-00229-y.

Kim, K. H., J. B. Kim, J. H. Ji, S. B. Lee, and G. N. Bae. 2015. "Nanoparticle Formation in a Chemical Storage Room as a New Incidental Nanoaerosol Source at a Nanomaterial Workplace." *Journal of Hazardous Materials* 298: 36–45. doi:10.1016/j.jhazmat.2015.05.002

Kuuluvainen, H., T. Ronkko, A. JarvineN, S. Saari, P. Karjalainen, T. Lahde, L. Pirjola, et al. 2016. "Lung Deposited Surface Area Size Distributions of Particulate Matter in Different Urban Areas." *Atmospheric Environment* 136: 105–113. doi:10.1016/j.atmosenv.2016.04.019.

Li, M., Y. Liu, G. Zeng, N. Liu, and S. Liu. 2019. "Graphene and Graphene-Based Nanocomposites Used for Antibiotics Removal in Water Treatment: A Review." *Chemosphere* 226: 360–380. doi:10.1016/j.chemosphere.2019.03.117

Malvindi, M. A., V. Brunetti, G. Vecchio, A. Galeone, R. Cingolani, and P. P. Pompa. 2012. "SiO₂ Nanoparticles Biocompatibility and Their Potential for Gene Delivery and Silencing." *Nanoscale* 4 (2): 486–495. doi:10.1039/c1nr11269d

Malvindi, M. A., V. De Matteis, A. Galeone, V. Brunetti, G. C. Anyfantis, A. Athanassiou, R. Cingolani, et al. 2014. "Toxicity Assessment of Silica Coated Iron Oxide Nanoparticles and Biocompatibility Improvement by Surface Engineering." *PloS One* 9 (1): e85835. doi:10.1371/journal.pone.0085835

Q10

Q5

Q6

Q7

Q4

1844
1845
1846
1847
1848
1849
1850
1851
1852
1853
1854
1855
1856
1857
1858
1859
1860
1861
1862
1863
1864
1865
1866
1867
1868
1869
1870
1871
1872
1873
1874
1875
1876
1877
1878
1879
1880
1881
1882
1883
1884
1885
1886
1887
1888
1889
1890
1891

1892
1893
1894
1895
1896
1897
1898
1899
1900
1901
1902
1903
1904
1905
1906
1907
1908
1909
1910
1911
1912
1913
1914
1915
1916
1917
1918
1919
1920
1921
1922
1923
1924
1925
1926
1927
1928
1929
1930
1931
1932
1933
1934
1935
1936
1937
1938
1939
1940

- Murugadoss, S., D. Lison, L. Godderis, S. Van Den Brule, J. Mast, F. Brassinne, N. Sebaihi, et al. 2017. "Toxicology of Silica Nanoparticles: An update." *Archives of Toxicology* 91 (9): 2967–3010. doi:10.1007/s00204-017-1993-y
- Novoselov, K. S., A. K. Geim, S. V. Morozov, D. Jiang, Y. Zhang, S. V. Dubonos, I. V. Grigorieva, et al. 2004. "Electric Field Effect in Atomically Thin Carbon Films." *Science (New York, N.Y.)* 306 (5696): 666–669. doi:10.1126/science.1102896.
- Oberdorster, G., E. Oberdorster, and J. Oberdorster. 2005. "Nanotoxicology: An Emerging Discipline Evolving from Studies of Ultrafine Particles." *Environmental Health Perspectives* 113: 823–839. doi:10.1289/ehp.7339.
- Organization for Economic Cooperation and Development (OECD). 2015. "Harmonized Tiered Approach to Measure and Assess the Potential Exposure to Airborne Emissions of Engineered Nano-Objects and Their Agglomerates and Aggregates at Workplaces." ENV/JM/MONO(2015)19. Accessed 5 June 2020. [http://www.oecd.org/officialdocuments/publicdisplaydocumentpdf/?cote=env/jm/mono\(2015\)19&doclanguage=en](http://www.oecd.org/officialdocuments/publicdisplaydocumentpdf/?cote=env/jm/mono(2015)19&doclanguage=en)
- Organization for Economic Cooperation and Development (OECD). 2017. "Strategies, Techniques and Sampling Protocols for Determining the Concentrations of Manufactured Nanomaterials in Air at the Workplace". ENV/JM/MONO(2017)30. Accessed 5 June 2020. [http://www.oecd.org/officialdocuments/publicdisplaydocumentpdf/?cote=env/jm/mono\(2017\)30&doclanguage=en](http://www.oecd.org/officialdocuments/publicdisplaydocumentpdf/?cote=env/jm/mono(2017)30&doclanguage=en)
- Pacheco-Torgal, F., M. V. Diamanti, A. Nazari, C. G. Granqvist, A. Pruna, and S. Amirkhanian. 2019. *Nanotechnology in Eco-Efficient Construction*. 2nd ed. Duxford, UK: Woodhead Publishing by Elsevier.
- Ramachandran, G., and D. W. Cooper. 2011. "Size Distribution Data Analysis and Presentation." In *Aerosol Measurement*, edited by P. Kullarni P.A. Baron and K. Willeke, 479–506. 3rd ed. Hoboken, NJ: John Wiley.
- Schinwald, A., F. A. Murphy, A. Jones, W. MacNee, and K. Donaldson. 2012. "Graphene-Based Nanoplatelets: A New Risk to the Respiratory System as a Consequence of Their Unusual Aerodynamic Properties." *ACS Nano* 6 (1): 736–746. doi:10.1021/nn204229f
- Schulte, P., V. Leso, M. Niang, and I. Iavicoli. 2018. "Biological Monitoring of Workers Exposed to Engineered Nanomaterials." *Toxicology Letters* 298: 112–124. doi:10.1016/j.toxlet.2018.06.003
- Schulte, P. A., V. Leso, M. Niang, and I. Iavicoli. 2019. "Current State of Knowledge on the Health Effects of Engineered Nanomaterials in Workers: A Systematic Review of Human Studies and Epidemiological Investigations." *Scandinavian Journal of Work, Environment & Health* 45 (3): 217–238. doi:10.5271/sjweh.3800
- Shvedova, A. A., N. Yanamala, E. R. Kisin, T. O. Khailullin, M. E. Birch, and L. M. Fatkhutdinova. 2016. "Integrated Analysis of Dysregulated ncRNA and mRNA Expression Profiles in Humans Exposed to Carbon Nanotubes." *PLoS One* 11 (3): e0150628. doi:10.1371/journal.pone.0150628
- Tombolini, F., F. Boccuni, R. Ferrante, C. Natale, L. Marasco, E. Mantero, A. E. Del Rio Castillo, et al. 2020. "Integrated and Multi-Technique Approach to Characterize Airborne Graphene Flakes in the Workplace Exposure During the Production Phases". Submitted for publication in *Nanoscale*.
- Ursini, C. L., A. M. Freseghna, A. Ciervo, R. Maiello, V. Del Frate, D. Poli, G. Folesani, et al. 2020. "Occupational Exposure to Graphene and Silica Nanoparticles. Part II: Pilot Study to Identify a Panel of Sensitive Biomarkers of Genotoxic, Oxidative and Inflammatory Effects on Suitable Biological Matrices". Submitted for publication in *Nanotoxicology*.
- World Health Organization (WHO). 2017. *Guidelines on Protecting Workers from Potential Risks of Manufactured Nanomaterials*. Geneva, Switzerland: WHO.
- Yeganeh, B., C. M. Kull, M. S. Hull, and L. C. Marr. 2008. "Characterization of Airborne Particles During Production of Carbonaceous nanomaterials." *Environmental Science & Technology* 42 (12): 4600–4606. doi:10.1021/es703043c

1989
1990
1991
1992
1993
1994
1995
1996
1997
1998
1999
2000
2001
2002
2003
2004
2005
2006
2007
2008
2009
2010
2011
2012
2013
2014
2015
2016
2017
2018
2019
2020
2021
2022
2023
2024
2025
2026
2027
2028
2029
2030
2031
2032
2033
2034
2035
2036
2037